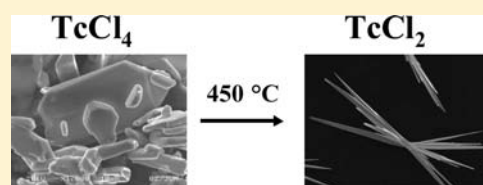


## Technetium Tetrachloride Revisited: A Precursor to Lower-Valent Binary Technetium Chlorides

Erik V. Johnstone,<sup>\*,†</sup> Frederic Poineau,<sup>†</sup> Paul M. Forster,<sup>†</sup> Longzou Ma,<sup>‡</sup> Thomas Hartmann,<sup>‡</sup> Andrew Cornelius,<sup>§</sup> Daniel Antonio,<sup>§</sup> Alfred P. Sattelberger,<sup>†,⊥</sup> and Kenneth R. Czerwinski<sup>†</sup><sup>†</sup>Department of Chemistry, <sup>‡</sup>Harry Reid Center for Environmental Studies, and <sup>§</sup>Department of Physics and Astronomy, University of Nevada—Las Vegas, Las Vegas, Nevada 89154, United States<sup>⊥</sup>Energy Engineering and Systems Analysis Directorate, Argonne National Laboratory, Argonne, Illinois 60439, United States

## Supporting Information

**ABSTRACT:** Technetium tetrachloride has been prepared from the reaction of technetium metal with excess chlorine in sealed Pyrex ampules at elevated temperatures. The product was characterized by single-crystal and powder X-ray diffraction, transmission electron microscopy, scanning electron microscopy, and alternating-current magnetic susceptibility. Solid  $\text{TcCl}_4$  behaves as a simple paramagnet from room temperature down to 50 K with  $\mu_{\text{eff}} = 3.76 \mu_{\text{B}}$ . Below 25 K,  $\text{TcCl}_4$  exhibits an antiferromagnetic transition with a Néel temperature ( $T_{\text{N}}$ ) of  $\sim 24$  K. The thermal behavior of  $\text{TcCl}_4$  was investigated under vacuum at 450 °C; the compound decomposes stepwise to  $\alpha\text{-TcCl}_3$  and  $\text{TcCl}_2$ .



## INTRODUCTION

Transition-metal tetrahalides exhibit a wide range of structural and physical properties.<sup>1,2</sup> For technetium, the last transition-metal discovered and the lightest radioelement, two tetrahalides ( $\text{TcCl}_4$  and  $\text{TcBr}_4$ ) have been reported.<sup>3,4</sup> In comparison, its heavier congener, rhenium, forms tetrahalides with fluorine, chlorine, bromine, and iodine.<sup>5–8</sup> Of the second-row transition metals, technetium is the last element in the series to form an isolable, structurally characterized tetrachloride. Technetium tetrachloride was first reported over 50 years ago; it was synthesized from the reaction of  $\text{Tc}_2\text{O}_7$  with  $\text{CCl}_4$  in a pressure vessel or by flowing chlorine gas over the metal at elevated temperatures.<sup>9,10</sup> Technetium tetrachloride was the first tetrahalide of group 7 to be structurally characterized. Its structure, significantly different from that of  $\text{ReCl}_4$  (vide infra),<sup>11</sup> consists of infinite chains of edge-sharing  $\text{TcCl}_6$  octahedra. Though the structure of technetium tetrachloride has been determined, there is a discrepancy between the two sets of cell parameters published for this compound.<sup>12,13</sup> Theoretical calculations on the structure and properties of  $\text{TcX}_4$  ( $X = \text{Cl}, \text{F}, \text{Br}, \text{I}$ ) have been performed. The results on  $\text{TcCl}_4$  indicate that the calculated  $\text{Tc}-\text{Cl}$  distances are within  $\sim 1\%$  of the published experimental values.<sup>14</sup> Previous studies of  $\text{TcCl}_4$  gave an effective magnetic moment of  $3.14 \mu_{\text{B}}$ .<sup>15</sup> This value is significantly lower than the theoretical one, viz.,  $3.87 \mu_{\text{B}}$ , expected for a spin-only  $d^3$  paramagnet. The magnetic results and lack of characterization raises questions about the sample purity of bulk  $\text{TcCl}_4$ .<sup>15</sup> To the best of our knowledge, neither a powder X-ray diffraction (XRD) pattern nor any microscopy characterization have been reported for  $\text{TcCl}_4$ . The chemistry of  $\text{TcCl}_4$  is also sparse. It forms a number of octahedral adducts of the type  $\text{TcCl}_4(\text{L})_2$  with various monodentate donor ligands  $\text{L}$  in solution, but there are no reports on its thermal stability at

elevated temperatures.<sup>16</sup> For other transition-metal tetrahalides, thermal decomposition and/or disproportionation often occurs.<sup>17,18</sup> Because of the recent discoveries of  $\text{TcCl}_2$  and  $\alpha$ - and  $\beta\text{-TcCl}_3$ ,  $\text{TcCl}_4$  seemed a likely precursor to the technetium(II) or -(III) chlorides.<sup>19–21</sup> Here, we report a new method for the preparation of  $\text{TcCl}_4$  and its characterization by scanning electron microscopy (SEM), energy-dispersive X-ray spectroscopy (EDS), magnetic susceptibility, and powder XRD. Its solid-state structure has also been redetermined by single-crystal XRD (SCXRD). Finally, the thermal stability of  $\text{TcCl}_4$  was investigated, and its decomposition products were characterized.

## EXPERIMENTAL SECTION

**Caution!** Technetium-99 is a weak  $\beta$ -emitter ( $E_{\text{max}} = 292$  keV). All manipulations were performed in a laboratory designed for work with radionuclides using efficient HEPA-filtered fume hoods and Schlenk and glovebox techniques and following locally approved radiochemistry handling and monitoring procedures. Laboratory coats, disposable gloves, and protective eyewear were worn at all times.

**Syntheses. Reagents.** Technetium metal was prepared by hydrogen reduction of  $\text{TcO}_2$  at 750 °C (2 h) under an  $\text{Ar}/\text{H}_2$  (5%) atmosphere as described previously.<sup>3</sup> A lecture bottle of  $\text{Cl}_2$  was purchased from Sigma-Aldrich and used as received.

**Preparation of Technetium Tetrachloride.** Technetium metal (20.1 mg, 0.203 mmol) was placed in a Pyrex tube (o.d. = 10 mm, i.d. = 7 mm, and  $L = 43$  cm), and the tube was connected to a Schlenk line and flamed under vacuum. After backfilling with chlorine gas ( $\text{Tc}:\text{Cl}$ ,  $\sim 1:6$ ) at ambient temperature and pressure, the tube was isolated from the Schlenk line and the lower end of the tube was cooled in liquid nitrogen to condense the chlorine. The tube was flame-sealed ( $L = 18$

Received: May 15, 2012

Published: July 9, 2012

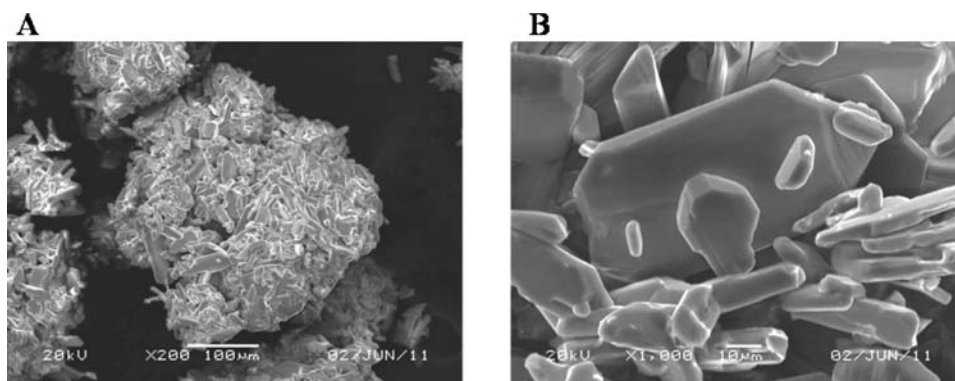


**Figure 1.** SEM images of the  $\text{TcCl}_4$  powder: (A)  $\times 200$ ; (B)  $\times 1000$ .

cm) and placed in a open-ended quartz tube packed with glass wool at each end. The tubes were inserted into a Thermo Fisher Scientific Lindberg/Blue M Mini-Mite 1100 °C clamshell furnace with the metal end of the sealed tube located in the center of the furnace. The temperature was increased to 450 °C at 7.5 °C/min and held at that temperature for 14 h. After cooling to room temperature, a reddish-black crystalline powder was observed at the cool end of the tube together with a red amorphous film. The crystalline powder was removed, placed in a second Pyrex tube of identical dimensions as the first, sealed under a Cl atmosphere, and reacted as before. The reddish-black powder (33.8 mg, 69%) and several small red needles (~1 mg) in the middle of the tube were recovered.

**Thermal Decomposition of Technetium Tetrachloride to Technetium Dichloride.** A sample of  $\text{TcCl}_4$  (39.5 mg, 0.164 mmol) was placed in a 30-cm-long Pyrex tube, and the tube was then evacuated and sealed at 18 cm. The tube was placed in a tube furnace for 14 h at 450 °C with the solid at the center of the furnace. After cooling to room temperature, the reaction yielded a black crystalline powder (6.2 mg) at one end of the tube, lustrous black needles in the middle, and a black amorphous film at the coolest end. The resulting products were analyzed by XRD and SEM.

**Thermal Decomposition of Technetium Tetrachloride to Technetium Trichloride.** A sample of  $\text{TcCl}_4$  powder (23.2 mg, 0.096 mmol) was placed in a 30-cm-long Pyrex tube, and the tube was then evacuated, sealed at 18 cm, and reacted for 2 h at 450 °C. After the reaction, red needles and small purple hexagonal plates were located near the center of the tube, an amorphous black film was observed at the coolest end of the tube, and no remaining product was seen at the hottest portion of the tube.

**Characterization Methods.** SCXRD data were collected on a Bruker Apex II system equipped with an Oxford nitrogen cryostream operating at 100 K. Crystals were mounted under Paratone on a glass fiber. Data processing was performed using the *Apex II* suite of programs, and an absorption correction was performed with *SADABS*. Structure determination (direct methods) and refinement were carried out using *SHELX97*.<sup>22</sup>

The powder XRD patterns were obtained using a Bruker D8 Advance diffractometer employing  $\text{Cu K}\alpha_1$  X-rays from 10 to 120° ( $2\theta$ ) with a step size of 0.008° ( $2\theta$ ) and 0.65 s/step. The powder XRD patterns were quantified by a Le Bail fit using the *Topas 4.0* software. The samples (~10–20 mg) were ground in an agate mortar, dispersed on a low-background silicon disk sample holder, covered with a radiological containment dome, and placed in the instrument for measurement.

SEM imaging was performed on a JEOL scanning electron microscope model JSM-5610 equipped with secondary electron and backscattered electron detectors. EDS was performed on a TECNAI-G2-F30 Supertwin transmission electron microscope with a 300 keV field emission gun. The elemental composition of the sample was analyzed using the energy-dispersive X-ray spectroscope under the scanning transmission electron microscopy (STEM) mode. For the STEM/EDS mode, a 0.2 nm electron probe was used to examine a dedicated area of the sample. The transmission electron microscopy

(TEM) samples were prepared by a solution-drop method. A total of 2–5 mg of the sample material was ground with hexane in an agate mortar. After slight shaking, one drop of the suspension was placed onto a 3-mm-diameter carbon-coated copper grid using a small-tipped transfer pipet. The liquid was evaporated at room temperature, leaving the fine particulate sample deposited on the carbon film.

Magnetic measurements were performed in a 0.1 T applied field from 10 to 300 K using a Quantum Design PPMS. The sample was prepared by placing a weighted quantity of powder (34.1 mg, 0.142 mmol) in the bottom of a medical capsule packed with cotton. The capsule was wrapped and sealed with Kapton tape and firmly inserted into the bottom of a plastic straw, which was fitted onto the sample holder.

## RESULTS AND DISCUSSION

**Synthesis of Technetium Tetrachloride.** Technetium tetrachloride was synthesized in a sealed glass ampule from the elements at elevated temperature. A subsequent treatment of the resulting powder with excess chlorine at 450 °C for 14 h was required to yield pure, single crystalline  $\text{TcCl}_4$  phase. In comparison to the flowing gas system, sealed tube reactions give somewhat lower yields but avoid the generation of volatile technetium oxychlorides (i.e.,  $\text{TcO}_3\text{Cl}$  and  $\text{TcOCl}_4$ ), which are observed even in the presence of low-oxygen-content chlorine streams.<sup>23</sup> It also represents a safe, convenient way to handle and manipulate small quantities of a volatile radioactive sample.

The behavior of elemental technetium in a Cl atmosphere can be compared to that of other second- and third-row transition metals. Tetrachlorides are obtained directly from the reactions of chlorine with zirconium,<sup>24</sup> hafnium,<sup>24</sup> osmium,<sup>25,26</sup> and platinum metal.<sup>27</sup> Reacting molybdenum metal and excess chlorine yields  $\text{MoCl}_5$ .  $\beta$ - $\text{MoCl}_4$  is obtained from the reaction of the pentachloride with  $\text{MoCl}_3$  in a sealed tube at 250 °C,<sup>28</sup> while the  $\alpha$  phase is synthesized by refluxing  $\text{MoCl}_5$  with tetrachloroethylene and carbon tetrachloride.<sup>29</sup> Chlorination of tungsten metal yields  $\text{WCl}_6$ , which can then be reduced with aluminum to form the tetrachloride.<sup>30</sup> For rhenium, the direct chlorination of the metal results in a mixture of  $\text{ReCl}_5$  and  $\text{ReCl}_6$ .<sup>10,31</sup> Two phases have been identified for  $\text{ReCl}_4$ :  $\beta$ <sup>32</sup> and  $\gamma$ .<sup>33</sup> The  $\beta$  phase, which is the only structurally characterized phase, was obtained via the reaction of  $\text{ReCl}_5$  with either  $\text{ReCl}_3$  or  $\text{SbCl}_3$ .<sup>11</sup> Ruthenium and rhodium trichlorides are both formed from the reaction of the elements, and neither element forms a stable binary chloride in the 4+ oxidation state.<sup>34,35</sup>

**Characterization of Technetium Tetrachloride.** The energy-dispersive X-ray (EDS) spectrum of  $\text{TcCl}_4$  (Figure S1 in the Supporting Information) shows the presence of the Tc  $K\alpha$ , Tc  $L\alpha$ , and Cl  $K\alpha$  lines, confirming the formation of a binary

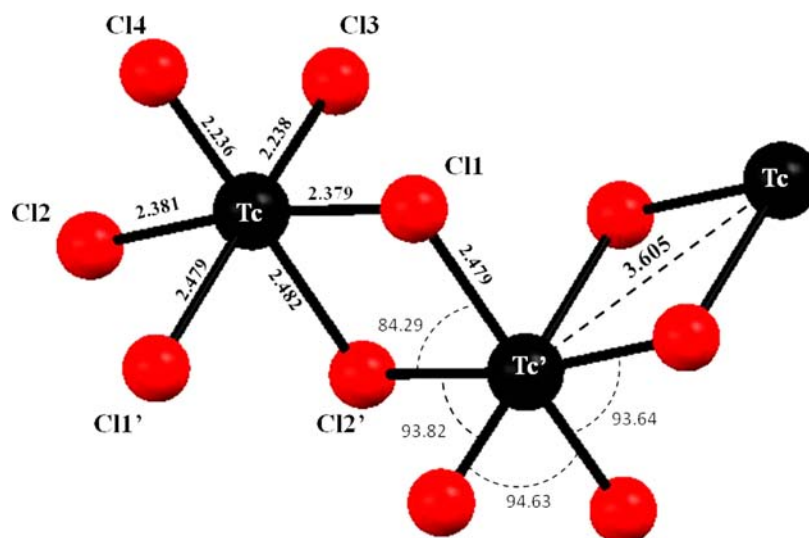


**Figure 2.** Ball-and-stick representation of  $\text{TcCl}_4$ . Two edge-sharing octahedra and a portion of a third octahedron are represented. Distances are in Å and angles in degrees.

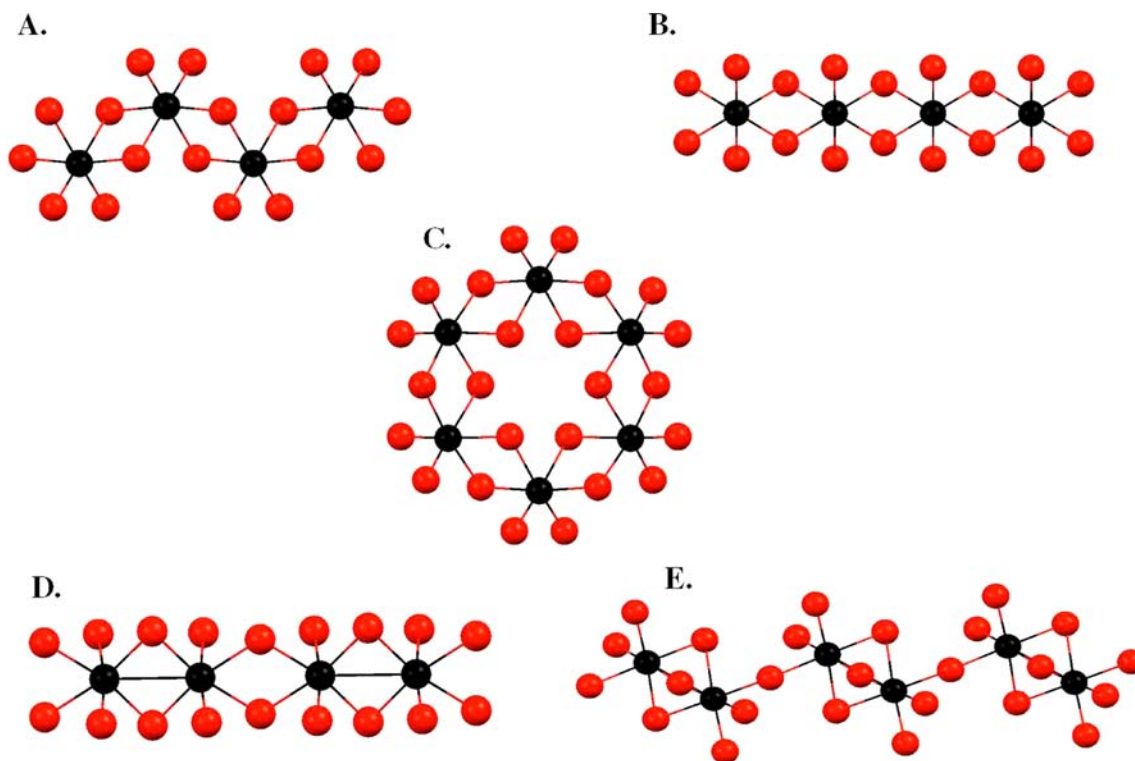


**Figure 3.** Ball-and-stick representations of second- and third-row transition-metal tetrachloride structure types: (A) zirconium, hafnium, technetium, and platinum; (B) osmium; (C)  $\beta$ -molybdenum; (D) niobium, tantalum,  $\alpha$ -molybdenum, and tungsten; (E)  $\beta$ -rhenium. The metal atoms are in black, and the chlorine atoms are in red.

chloride. The integrated areas of the Cl  $K\alpha$  and Tc  $K\alpha$  peaks were used to calculate an atomic ratio of chlorine to technetium of 3.99(5). The XRD pattern (Figure S2 in the Supporting Information) shows a single crystalline  $\text{TcCl}_4$  phase and the absence of technetium metal. A Le Bail fit of the powder XRD pattern confirms that the compound crystallizes at room temperature in the  $Pbca$  space group with lattice parameters  $a = 6.0258(5)$  Å,  $b = 11.6460(4)$  Å, and  $c = 14.0289(1)$  Å. A Reitveld analysis of the pattern gave a less satisfactory fit because of the strong texture within the sample.

An SEM image (Figure 1) reveals the morphology of the tetrachloride as being a combination of small rods and larger rectangular plates ranging in size from 10 to 100  $\mu\text{m}$ . These crystalline rods and plates are typically found in clusters throughout the powder. After thermal decomposition of  $\text{TcCl}_4$ , the rods contained in the initial powder source are transformed into the crystals with other morphologies.

The structure of  $\text{TcCl}_4$  was redetermined by SCXRD. Single crystals are grown in the presence of a Cl atmosphere as a phase transport agent within a sealed Pyrex tube. In agreement with previous results,  $\text{TcCl}_4$  crystallizes in the orthorhombic

space group  $Pbca$  and consists of infinite ordered zigzag chains of edge-sharing  $TcCl_6$  octahedra (Figure 2).<sup>13,14</sup> Technetium tetrachloride is isostructural with  $PtCl_4$ <sup>36</sup> and  $TcBr_4$ .<sup>5</sup> The cell parameters at 100 K are  $a = 6.0111(4)$  Å,  $b = 11.5308(9)$  Å, and  $c = 13.9334(10)$  Å. The  $Tc\cdots Tc$  separation of  $3.6048(3)$  Å within the chain precludes any direct metal–metal bonding. Within a given octahedron, three different  $Tc-Cl$  distances are observed. The shortest distance is attributed to the two cis terminal chlorines, Cl3 and Cl4 (av  $Tc-Cl = 2.2368[6]$  Å). The other two distances are associated with two different sets of bridging chlorine atoms. Of these, the bonded chlorine atoms Cl1' and Cl2' perpendicular to the chain are the longest (av  $Tc-Cl = 2.4808[6]$  Å), whereas the chlorine atoms Cl1 and Cl2 parallel to the chain are slightly shorter (av  $Tc-Cl = 2.3797[6]$  Å). Atomic coordinates and additional structural parameters are provided in the Supporting Information.

**Comparison with Other  $MCl_4$  Systems.** Five different structure types have been identified for the second- and third-row transition-metal tetrachlorides spanning groups 4–10 ( $d^0-d^6$ ) for zirconium, hafnium, niobium, tantalum, molybdenum, tungsten, technetium, rhenium, osmium, and platinum. These tetrachlorides are comprised of  $MCl_6$  edge- or face-sharing octahedra, forming either infinite chains or layered sheets (Figure 3). These compounds can be differentiated based on the presence or absence of metal–metal bonding.

The structure types in Figure 3A–C are representative of transition-metal tetrachlorides that exhibit no metal–metal bonding. Similar to technetium, the tetrachlorides of zirconium,<sup>37</sup> hafnium,<sup>38</sup> and platinum<sup>36</sup> (Figure 3A) adopt the “ $TcCl_4$ ” structure type. The  $M-M$  separations within the chains suggest little or no interaction between neighboring metal ions. The  $OsCl_4$ <sup>39</sup> structure type (Figure 3B) consists of infinite linear chains of edge-sharing  $OsCl_6$  octahedra with a single  $Os\cdots Os$  separation of  $3.56(1)$  Å, suggesting the absence of metal–metal bonding. The  $\beta-MoCl_4$ <sup>40</sup> structure type consists of infinite layered sheets instead of chains of  $MCl_6$  octahedra (Figure 3C). The  $Mo\cdots Mo$  separation in this structure,  $3.670(1)$  Å, also precludes any metal–metal bonding.

The structure types for the transition-metal tetrachlorides that can be classified as metal–metal bonded are shown in Figure 3D,E and Table 1. The  $NbCl_4$ <sup>41</sup> structure type (Figure 3D) is also found for  $TaCl_4$ ,<sup>42</sup>  $\alpha-MoCl_4$ ,<sup>29</sup> and  $WCl_4$ .<sup>30</sup> These compounds consist of edge-sharing chains of distorted  $MCl_6$  octahedra with alternating short and long metal–metal distances. The shorter distances suggest the presence of some metal–metal interaction.  $\beta$ -Rhenium tetrachloride (Figure 3E) consists of infinite chains of distorted  $Re_2Cl_9$  confacial biotetrahedra linked by a terminal chlorine atom. In the  $Re_2Cl_9$  unit, the  $Re-Re$  separation [i.e.,  $2.728(2)$  Å] is indicative of a strong metal–metal interaction.

Previous magnetic susceptibility measurements were recorded on a sample of  $TcCl_4$  prepared from the reaction of  $Tc_2O_7$  with  $CCl_4$ .<sup>15</sup> No measurements have been performed on a sample of  $TcCl_4$  synthesized from the reaction of the metal with chlorine gas, and no magnetic data have been collected below 78 K. A plot of the magnetic susceptibility versus temperature (Figure 4) shows features typical of an antiferromagnet with a cusp indicating the Néel temperature ( $T_N$ ) at about 24 K and of a paramagnet above  $T_N$ . A fit of the data (Figure S2 in the Supporting Information) above 50 K to the Curie–Weiss law:  $\chi = C/(T + \theta) + \chi_0$  gives a Curie temperature of  $\theta = 51(1)$  K and a diamagnetic contribution of  $\chi_0 = -3.1(8) \times 10^{-4}$  emu/mol. The effective moment at each

**Table 1. Structure Types and Metal–Metal Separations in Transition-Metal Tetrachlorides**

electronic configuration	metal	structure type	M–M and M $\cdots$ M (in italics) distances (Å)
$d^0$	Zr	$TcCl_4$ (Figure 3A)	3.962(1)
	Hf	$TcCl_4$	3.920(1)
$d^1$	Nb	$NbCl_4$ (Figure 3D)	3.029(2), 3.794(2)
	Ta	$NbCl_4$	2.985(3), 3.791(3)
$d^2$	Mo	$\alpha$ : $NbCl_4$ $\beta$ : $MoCl_4$ (Figure 4C)	<i>b</i> 3.670(1)
	W	$NbCl_4$	2.688(1), 3.787(1)
$d^3$	Tc	$TcCl_4$	3.604(8)
	Re	$\beta$ : $ReCl_4$ (Figure 4E)	2.728(2), 4.368(2)
$d^4$	Ru	<i>a</i>	<i>a</i>
	Os	$OsCl_4$ (Figure 3B)	3.560(1)
$d^5$	Rh	<i>a</i>	<i>a</i>
	Ir	<i>a</i>	<i>a</i>
$d^6$	Pd	<i>a</i>	<i>a</i>
	Pt	$TcCl_4$	<i>b</i>

<sup>a</sup>Not reported. <sup>b</sup>Characterized by powder XRD and interatomic distances not reported.

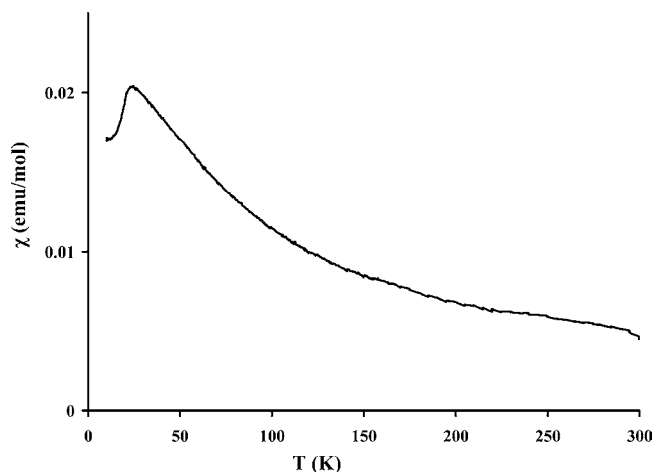


**Figure 4.** Magnetic susceptibility as a function of the temperature for  $TcCl_4$ . Measurement performed between 10 and 300 K on a 34.1 mg sample in a 0.1 T magnetic field.

$Tc$  site is then  $\mu_{\text{eff}} = (3Ck_B/N)^{1/2} = 3.76(3) \mu_B$ . In comparison to the previously measured value of  $3.14 \mu_B$ ,<sup>15</sup> this measurement is much closer to the theoretical, spin-only value (i.e., the orbital angular momentum is effectively zero) of  $3.87 \mu_B$ . This moment is similar to the one found in other  $4d^3$  species, i.e.,  $K_2TcCl_6$  ( $4.05 \mu_B$ )<sup>43</sup> and  $K_3MoCl_6$  ( $3.79 \mu_B$ ).<sup>44</sup> The magnetic behavior for  $TcCl_4$  is similar to the one expected for an isolated  $Tc^{(IV)}Cl_6$  octahedron and is consistent with the absence of a significant metal–metal interaction in  $TcCl_4$ .<sup>15</sup>

**Thermal Behavior of Technetium Tetrachloride.** The thermal behavior of  $TcCl_4$  was studied in a flow system in the presence of argon and in a sealed tube under vacuum at  $450$  °C. The latter temperature is one that we previously employed for the synthesis of lower-valent binary technetium chlorides.<sup>19,21</sup> Experiments under flowing argon at  $250$ – $500$  °C for 14 h only resulted in volatilization of the starting material.

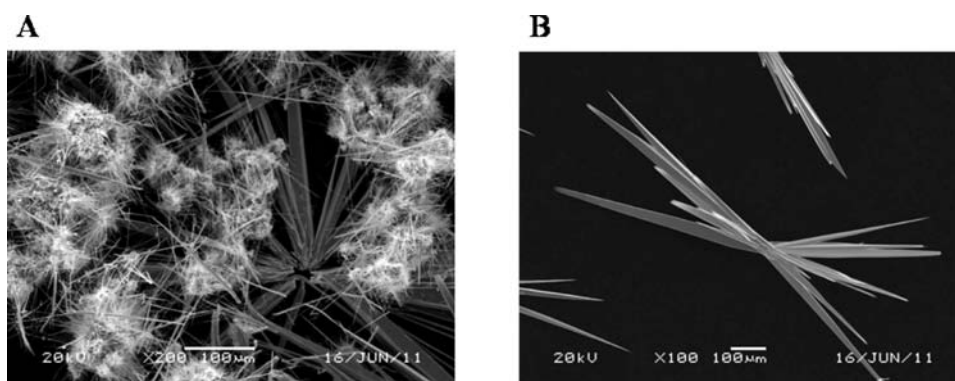


Figure 5. SEM images of the powder (A,  $\times 200$ ) and crystals (B,  $\times 100$ ) obtained after decomposition of  $\text{TcCl}_4$  at  $450^\circ\text{C}$  under vacuum for 14 h.

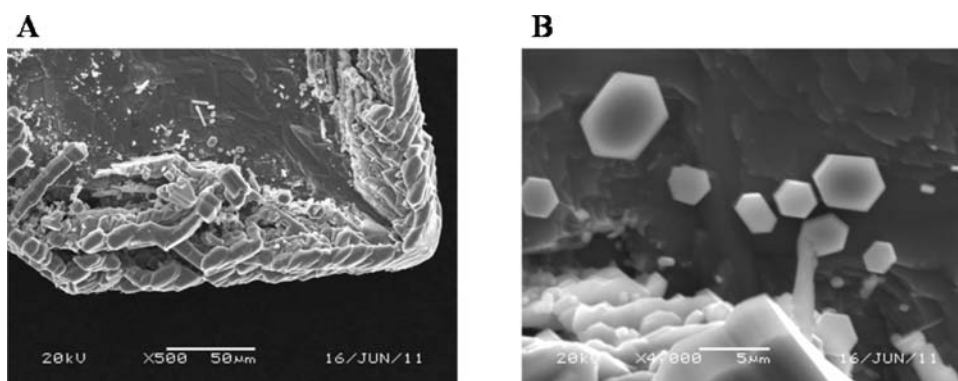


Figure 6. SEM images of the surface of a  $\text{TcCl}_4$  crystal (A,  $\times 500$ ; B,  $\times 4000$ ) obtained after decomposition of  $\text{TcCl}_4$  at  $450^\circ\text{C}$  under vacuum for 2 h.

**Decomposition of  $\text{TcCl}_4$  under Vacuum.** In a first experiment,  $\text{TcCl}_4$  was reacted at  $450^\circ\text{C}$  for 14 h. After the reaction, a dark black powder, needlelike crystals (center of the tube), and a black amorphous film (cold end of the tube) were observed. The powder XRD of the black powder indicates the presence of both  $\text{TcCl}_4$  and  $\text{TcCl}_2$ . The needlelike single crystals were indexed by SCXRD, yielding cell parameters and a space group identical with that of  $\text{TcCl}_2$ . The structure of  $\text{TcCl}_2$  consists of infinite chains of face-sharing  $[\text{Tc}_2\text{Cl}_8]$  units.<sup>19</sup> SEM analysis of the powder (Figure 5A) and single crystal (Figure 5B) show the “sea urchin” cluster arrangement of the needle-shaped crystals characteristic of  $\text{TcCl}_2$  morphology.

In a second experiment,  $\text{TcCl}_4$  was reacted at  $450^\circ\text{C}$  in a sealed tube under vacuum for 2 h. After the reaction, red needles, small purple hexagonal plates, and an amorphous film were observed at the coolest end of the tube. The red needles were indexed using SCXRD as  $\text{TcCl}_4$ , while the purple hexagonal plates were indexed as  $\alpha\text{-TcCl}_3$  (i.e., space group  $R\bar{3}m$ ).<sup>20</sup> Analysis of the decomposition products by SEM (Figure 6A) shows the edge of a  $\text{TcCl}_4$  single crystal. Closer inspection of the  $\text{TcCl}_4$  crystal (Figure 6B) revealed the presence of small hexagonal crystals ( $2\text{--}5\ \mu\text{m}$ ) characteristic of  $\alpha$ -trichloride morphology.

It appears that the presence of a vacuum and elevated temperature is required for decomposition of  $\text{TcCl}_4$ . Decomposition provides two products in the early stages of the reaction, and the isolation of  $\alpha\text{-TcCl}_3$  after 2 h and  $\text{TcCl}_2$  after 14 h of reaction at  $450^\circ\text{C}$  suggests that the trichloride is likely the initial decomposition product.

In general, transition-metal tetrachlorides are thermally unstable; they can decompose or disproportionate as shown in Table 2. The thermal behavior of  $\text{TcCl}_4$  is similar to that of

Table 2. Summary of Transition-Metal Tetrachloride Decompositions

compound	conditions	products
$\beta\text{-MoCl}_4$	$288^\circ\text{C}$ , under argon	$\text{MoCl}_3$ and $\text{MoCl}_5$
$\text{WCl}_4$	$450\text{--}500^\circ\text{C}$ , vacuum	$\text{WCl}_2$ and $\text{WCl}_5$
$\text{TcCl}_4$	$450^\circ\text{C}$ , 2 h, vacuum	$\alpha\text{-TcCl}_3$
	$450^\circ\text{C}$ , 24 h, vacuum	$\text{TcCl}_2$
$\text{ReCl}_4$	$300^\circ\text{C}$ , under nitrogen	$\text{ReCl}_3$ and $\text{ReCl}_5$
$\text{OsCl}_4$	$470^\circ\text{C}$ , slight pressure of chlorine	$\text{OsCl}_3$
$\text{PtCl}_4$	$350^\circ\text{C}$ , open system with flowing $\text{N}_2(\text{g})$	$\text{Pt}_6\text{Cl}_{12}$

$\text{PtCl}_4$ , which also yields the dichloride as the final decomposition product.<sup>18</sup> Osmium tetrachloride decomposes to  $\text{OsCl}_3$  at  $470^\circ\text{C}$ .<sup>26,4</sup> In contrast,  $\text{ReCl}_4$  and  $\beta\text{-MoCl}_4$  undergo disproportionation to the respective tri- and pentachloride.<sup>31,32,45,46</sup> Tungsten(IV) chloride also disproportionates, forming  $\text{WCl}_2$  and  $\text{WCl}_5$ .<sup>47,30</sup> In comparison to the surrounding elements, technetium displays unique thermal properties upon undergoing successive decomposition to the tri- and dichlorides.

## CONCLUSION

Technetium tetrachloride was synthesized from the reaction of technetium metal with excess chlorine in sealed Pyrex tubes at elevated temperatures. The synthesis is preferred for small samples and avoids the formation of unwanted oxychlorides. The phase purity of the compound obtained by this method was analyzed by powder XRD, which confirmed the presence of a single crystalline  $\text{TcCl}_4$  phase. The structure of  $\text{TcCl}_4$  was revisited by SCXRD; more accurate structural parameters were obtained from this measurement. Magnetic measurements

confirmed  $\text{TcCl}_4$  to be paramagnetic above 50 K and to exhibit antiferromagnetic behavior below 24 K. The morphology of  $\text{TcCl}_4$  was observed by SEM as rod-shaped clusters and used to track compositional changes at various temperatures under vacuum. The thermal behavior of  $\text{TcCl}_4$  was investigated in sealed tubes under vacuum after 2 and 14 h at 450 °C. Diffraction and microscopic techniques show  $\text{TcCl}_4$  to decompose to  $\alpha\text{-TcCl}_3$  and  $\text{TcCl}_2$  after 2 h and to  $\text{TcCl}_2$  without a trace of the trichloride after 14 h;  $\alpha\text{-TcCl}_3$  appears to be the initial decomposition product, while  $\text{TcCl}_2$  is the ultimate thermodynamic product of decomposition under the prevailing experimental conditions.

The discovery of decomposition of  $\text{TcCl}_4$  to  $\alpha\text{-TcCl}_3$  and  $\text{TcCl}_2$  suggests that  $\text{TcBr}_4$  may also behave similarly. In this context, we note that technetium dibromide is still unknown. Similar studies are of interest for determining the possible existence of  $\text{ReCl}_2$ , i.e., via the thermal decomposition of  $\text{ReCl}_3$ . These experiments are in progress, and the results will be reported in due course.

## ■ ASSOCIATED CONTENT

### 📄 Supporting Information

Crystallographic tables and X-ray crystallographic data in CIF format for  $\text{TcCl}_4$ , EDX spectra of  $\text{TcCl}_4$ , and an additional magnetic measurement figure. This material is available free of charge via the Internet at <http://pubs.acs.org>.

## ■ AUTHOR INFORMATION

### Corresponding Author

\*E-mail: [erikjohnstone@gmail.com](mailto:erikjohnstone@gmail.com).

### Notes

The authors declare no competing financial interest.

## ■ ACKNOWLEDGMENTS

The authors thank Julie Bertoia and Trevor Low for outstanding laboratory management and health physics support. Funding for this project was supported by Department of Energy under the SISGR-Fundamental Chemistry of Technetium-99 Incorporated into Metal Oxide, Phosphate and Sulfide: Toward Stabilization of Low-Valent Technetium (Contract 47824B) and U.S. Department of Energy Award DE-SC0005278.

## ■ REFERENCES

- (1) Cotton, F. A.; Wilkinson, G.; Murillo, C. A.; Bochmann, M. *Advanced Inorganic Chemistry*, 6th ed.; John Wiley and Sons: New York, 1999.
- (2) Canterford, J. H.; Colton, R. *Halides of the Second and Third Row Transition Metals*; John Wiley and Sons: New York, 1968.
- (3) Poineau, F.; Rodriguez, E. E.; Forster, P. M.; Sattelberger, A. P.; Cheetham, A. K.; Czerwinski, K. R. *J. Am. Chem. Soc.* **2009**, *131*, 910–911.
- (4) Schwochau, K. *Technetium: Chemistry and Radiopharmaceutical Applications*; Wiley-VCH: Weinheim, Germany, 2000.
- (5) Peacock, R. D.; Welch, A. J. E.; Wilson, L. F. *J. Chem. Soc.* **1958**, 2901–2902.
- (6) Cotton, F. A.; DeBoer, B. G.; Mester, Z. *J. Am. Chem. Soc.* **1972**, *95*, 1159–1163.
- (7) Casteel, W. J.; Lohmann, D. H.; Bartlett, N. J. *Fluorine Chem.* **2001**, *112*, 165–171.
- (8) Mueller, H.; Waschinski, R. *Inorg. Nucl. Chem. Lett.* **1972**, *8*, 413–415.
- (9) Knox, K.; Tyree, S. Y., Jr.; Srivastava, R. D.; Norman, V.; Bassett, J. Y., Jr.; Holloway, J. H. *J. Am. Chem. Soc.* **1957**, *79*, 3358–3361.
- (10) Colton, R. *Nature* **1962**, *193*, 872–873.
- (11) Colton, R.; Martin, R. L. *Nature* **1965**, *205*, 239–240.
- (12) Elder, M.; Penfold, B. R. *Chem. Commun.* **1965**, 308–309.
- (13) Elder, M.; Penfold, B. R. *Inorg. Chem.* **1966**, *5*, 1197–1200.
- (14) Weck, P. F.; Kim, E.; Poineau, F.; Rodriguez, E. E.; Sattelberger, A. P.; Czerwinski, K. R. *Inorg. Chem.* **2009**, *48*, 6555–6558.
- (15) Knox, K.; Coffey, E. C. *J. Am. Chem. Soc.* **1958**, *81*, 5–7.
- (16) Hagenbach, A.; Yegan, E.; Abram, U. *Inorg. Chem.* **2006**, *45*, 7331–7338.
- (17) Fergusson, J. E.; Robinson, B. H.; Roper, W. R. *J. Chem. Soc.* **1962**, 2113–2115.
- (18) Degner, M.; Holle, B.; Kamm, J.; Pilbrow, M. F.; Thiele, G.; Wagner, D.; Weigl, W.; Wodtisch, P. *Transition Met. Chem.* **1976**, *1*, 41–47.
- (19) Poineau, F.; Malliakas, C. D.; Weck, P. F.; Scott, B. L.; Johnstone, E. V.; Forster, P. M.; Eunja, K.; Kanatzidis, M. G.; Czerwinski, K. R.; Sattelberger, A. P. *J. Am. Chem. Soc.* **2011**, *133*, 8814–8817.
- (20) Poineau, F.; Johnstone, E. V.; Weck, P. F.; Kim, E.; Forster, P. M.; Scott, B. L.; Sattelberger, A. P.; Czerwinski, K. R. *J. Am. Chem. Soc.* **2010**, *132*, 15864–15865.
- (21) Poineau, F.; Johnstone, E. V.; Weck, P. F.; Forster, P. M.; Kim, E.; Czerwinski, K. R.; Sattelberger, A. P. *Inorg. Chem.* **2012**, DOI: 10.1021/ic300612k.
- (22) Sheldrick, G. M. *Acta Cryst. A* **2008**, *64*, 112.
- (23) Guest, A.; Lock, C. J. L. *Can. J. Chem.* **1972**, *50*, 1807–1810.
- (24) Blumental, B. H. *The Chemical Behavior of Zirconium*; Van Nostrand: New York, 1958.
- (25) Ruff, O.; Bornemann, F. *Z. Anorg. Allg. Chem.* **1910**, *65*, 429–456.
- (26) Kolbin, N. I.; Semenov, I. N.; Shutov, Y. M. *Zh. Neorg. Khim.* **1963**, *8*, 2422–2427.
- (27) Wohler, L.; Streicher, S. *Ber. Dtsch. Chem. Ges.* **1913**, *46*, 1591–1597.
- (28) Couch, D. E.; Brenner, A. J. *Res. Natl. Bur. Std.* **1959**, *A63*, 185–188.
- (29) Kepert, D. L.; Mandyczewsky, R. *Inorg. Chem.* **1968**, *7*, 2091–2093.
- (30) McCarley, R. E.; Brown, T. M. *Inorg. Chem.* **1964**, *3*, 1232–1236.
- (31) Geilmann, W.; Wrigge, F. W.; Blitz, W. *Z. Anorg. Allgem. Chem.* **1933**, *214*, 244–247.
- (32) Frai, P. W.; Guest, A.; Lock, C. J. L. *Can. J. Chem.* **1969**, *47*, 1069–1072.
- (33) Brignole, A.; Cotton, F. A. *J. Chem. Soc., Chem. Commun.* **1971**, *13*, 706.
- (34) Fletcher, J. M.; Gardener, W. E.; Hooper, E. W.; Hyde, K. R.; Moore, F. H.; Woodhead, J. L. *Nature* **1963**, *199*, 1089–1090.
- (35) Puche, F. *Ann. Chim.* **1938**, *9*, 233–322.
- (36) Pilbrow, M. F. *J. Chem. Soc., Chem. Commun.* **1972**, *5*, 270–271.
- (37) Krebs, B. *Angew. Chem.* **1969**, *8*, 146–147.
- (38) Niewa, R.; Jacobs, H. *Z. Kristallogr.* **1995**, *210*, 687.
- (39) Cotton, F. A.; Rice, C. E. *Inorg. Chem.* **1977**, *16*, 1865–1867.
- (40) Müller, U. *Angew. Chem.* **1981**, *93*, 697–698.
- (41) Taylor, D. R.; Calabrese, J. C.; Larsen, E. M. *Inorg. Chem.* **1977**, *16*, 721–722.
- (42) Bajan, B.; Meyer, H. J. *Z. Kristallogr.* **1996**, *211*, 818.
- (43) Dalziel, J.; Gill, N. S.; Nyholm, R. S.; Peacock, R. D. *J. Chem. Soc.* **1958**, 4012–4016.
- (44) Figgis, B. N.; Lewis, J.; Mabbs, F. E. *J. Chem. Soc.* **1961**, 3138–3145.
- (45) Westland, A. D.; Uzelac, V. *Inorg. Chim. Acta* **1977**, *23*, L37–L39.
- (46) Larson, M. L.; Moore, F. W. *Inorg. Chem.* **1964**, *3*, 285–286.
- (47) Shchukarev, S. A.; Novikov, G. I.; Vasil'kova, I. V. *Zh. Neorg. Khim.* **1960**, *5*, 1650–1654.